



## In Situ Ionic/Electric Conductivity Measurement of $\text{La}_{0.55}\text{Li}_{0.35}\text{TiO}_3$ Ceramic at Different Li Insertion Levels

Chunsheng Wang,<sup>a,\*</sup> Prashanth Patil,<sup>b</sup> A. John Appleby,<sup>c,\*</sup> Frank. E. Little,<sup>d</sup> Mehmet Kesmez,<sup>b</sup> and David L. Cocke<sup>b,\*</sup>

<sup>a</sup>Center for Manufacturing Research and Department of Chemical Engineering, Tennessee Technological University, Cookeville, Tennessee 38505, USA

<sup>b</sup>Gill Chair Group of Chemistry and Chemical Engineering, Fuel Cell and Energy System Center, Lamar University, Beaumont, Texas 77710, USA

<sup>c</sup>Center for Electrochemical Systems and Hydrogen Research, Texas Engineering Experiment Station, Texas A&M University, College Station, Texas 77843-3402, USA

<sup>d</sup>Center for Space Power, Texas Engineering Experiment Station, Texas A&M University, College Station, Texas 77843-3118, USA

The electrical conductivities of solid  $\text{La}_{0.55}\text{Li}_{0.35}\text{TiO}_3$  electrolytes at different Li intercalation levels were measured, *in situ*, using a special cell and electrode design. The relative changes in electrical conductivities of  $\text{La}_{0.55}\text{Li}_{0.35}\text{TiO}_3$  at different Li insertion levels in liquid electrolytes were monitored by the voltage across the  $\text{La}_{0.55}\text{Li}_{0.35+x}\text{TiO}_3$  powder disk electrode sandwiched between two nickel screens and charged only on one nickel screen. The real electrical conductivities of the  $\text{La}_{0.55}\text{Li}_{0.35+x}\text{TiO}_3$  ceramic at different Li insertion levels  $x$  without influence of high-ion-conductivity liquid electrolytes was measured by electrochemical impedance spectroscopy using sintered  $\text{La}_{0.55}\text{Li}_{0.35+x}\text{TiO}_3$  disk electrodes with Au coating on both sides. Lithium was electrochemically inserted into  $\text{La}_{0.55}\text{Li}_{0.35}\text{TiO}_3$  when the Au coated disk electrodes were immersed into liquid electrolytes with the cell inverted. The impedances of  $\text{La}_{0.55}\text{Li}_{0.35+x}\text{TiO}_3$  electrodes were then measured with the disk electrode suspended above the liquid electrolyte with the cell upright.

© 2004 The Electrochemical Society. [DOI: 10.1149/1.1767157] All rights reserved.

Manuscript submitted September 2, 2003; revised manuscript received January 15, 2004. Available electronically June 25, 2004.

All-solid-state lithium-ion batteries have the advantages of high thermal stability, absence of leakage, resistance to shocks and vibrations, and possibly a wide electrochemical window. Their solid electrolytes should have high ionic conductivity. Some glass and ceramic materials, *e.g.*,  $\text{Li}_{1+x}\text{Al}_x\text{Ti}_2(\text{PO}_4)_3$  and  $\text{Li}_{0.5-3x}\text{La}_{0.5+x}\text{TiO}_3$  have ionic conductivities of the order of  $10^{-3}$  S/cm. However, these two compounds are unstable if they are directly used as solid electrolytes for the lithium-ion battery because they can intercalate Li atoms after electron transfer. This is followed by  $\text{Ti}^{4+}$  ion reduction with insertion of  $\text{Li}^+$  ion,<sup>1,2</sup> resulting in a change from Li-ion conductor (electronic insulator) to electronic conductor. A normal way to measure the electronic and ionic conductivity of  $\text{La}_{0.55}\text{Li}_{0.35+x}\text{TiO}_3$  as a function of Li content is to use samples with different Li compositions. However, this cannot reflect the real changes of electronic and ionic conductivity during Li insertion into ceramic electrolytes, which are not stable in air when their Li content is high. An improved method is to measure the conductivities of a sheet of  $\text{La}_{0.55}\text{Li}_{0.35+x}\text{TiO}_3$  in liquid electrolytes after electrochemically charging to different Li insertion levels. However, the ionic conductivity thus obtained can only reflect the relative conductivity change as Li content increases because the conductivity of liquid electrolytes is much higher than that of sintered  $\text{La}_{0.55}\text{Li}_{0.35+x}\text{TiO}_3$  sheet, resulting in short-circuiting, giving a higher conductivity than the real value under an inert atmosphere.

In this paper, the relative changes in electric conductivities of  $\text{La}_{0.55}\text{Li}_{0.35+x}\text{TiO}_3$  at different Li insertion levels in liquid electrolyte were monitored by the voltage across the  $\text{La}_{0.55}\text{Li}_{0.35+x}\text{TiO}_3$  powder disk electrodes sandwiched between two nickel screens and charged only on one of the nickel screens. The real electronic and ionic conductivity of  $\text{La}_{0.55}\text{Li}_{0.35+x}\text{TiO}_3$  without interference from liquid electrolyte after electrochemical insertion to different Li levels in a special poly(tetrafluoroethylene) (PTFE) cell was investigated for the first time by an *in situ* electrochemical method.

### Experimental

**Preparation of the electrode and the cell.**— $\text{La}_{0.55}\text{Li}_{0.35}\text{TiO}_3$  ceramic powders were prepared by mixing appropriate amounts of  $\text{La}_2\text{O}_3$  (99.9%, Alfa Aesar),  $\text{Li}_2\text{CO}_3$  (99%, Alfa Aesar), and  $\text{TiO}_2$  (99.9% Alfa Aesar), and then ballmilling in ethanol with stainless steel balls for 16 h. Two types of electrodes, sintered and powder sheet electrodes, were prepared. The sintered  $\text{La}_{0.55}\text{Li}_{0.35}\text{TiO}_3$  electrode sheets were used for electrical conductivity measurement at different Li insertion levels, and the  $\text{La}_{0.55}\text{Li}_{0.35}\text{TiO}_3$  powder electrodes were used to measure the relative electric conductivity during Li insertion by monitoring the voltage across the electrodes when they were charged/discharged on one side only using an Arbin (College Station, TX) automatic battery cycler. The sintered  $\text{La}_{0.55}\text{Li}_{0.35}\text{TiO}_3$  sheet electrode with a size of  $1 \times 1 \times 0.158$  cm was prepared by calcining a milled ceramic mixture at 800°C for 2 h and forming into a disk shape by die-pressing, followed by sintering at 1300°C for 4 h and then coating with Au on both sides, and pressing onto stainless steel sheets using stainless steel springs in a PTFE holder. The area of the stainless steel sheets is 1.8 cm<sup>2</sup>, which is larger than the sintered  $\text{La}_{0.55}\text{Li}_{0.35}\text{TiO}_3$  sheet. A special PTFE cell was constructed with a sintered  $\text{La}_{0.55}\text{Li}_{0.35}\text{TiO}_3$  disk electrode, and Li reference and counter electrodes, all suspended above a liquid electrolyte when the cell is in an upright position (Fig. 1). Li insertion/extraction into or from  $\text{La}_{0.55}\text{Li}_{0.35}\text{TiO}_3$  was conducted with the cell in inverted position, and the ionic conductivity of  $\text{La}_{0.55}\text{Li}_{0.35}\text{TiO}_3$  at the same Li content was measured by electrochemical impedance spectroscopy (EIS) in the absence of liquid electrolyte with the cell upright. When the cell is inverted, the electrode was completely immersed in liquid electrolyte with composition of 1.0 M  $\text{LiClO}_4$  in (1:1:1) EC-DEC-EMC.

$\text{La}_{0.55}\text{Li}_{0.35}\text{TiO}_3$  powder electrodes were prepared from a mixture of 92 wt % calcined  $\text{La}_{0.55}\text{Li}_{0.35}\text{TiO}_3$  (1100°C for 4 h) with 8 wt % polyvinylidene fluoride (PVDF) between two nickel screens current collectors using 1-methyl-2-pyrrolidinone as a solvent. The configuration of a typical powder electrode has been given in Fig. 2. The electrodes were put in a liquid electrolyte in a sealed PTFE cell with lithium reference and counter electrodes. The voltage differences across both sides being used to monitor their relative conductivity

\* Electrochemical Society Active Member.

<sup>z</sup> E-mail: cswang@tntech.edu

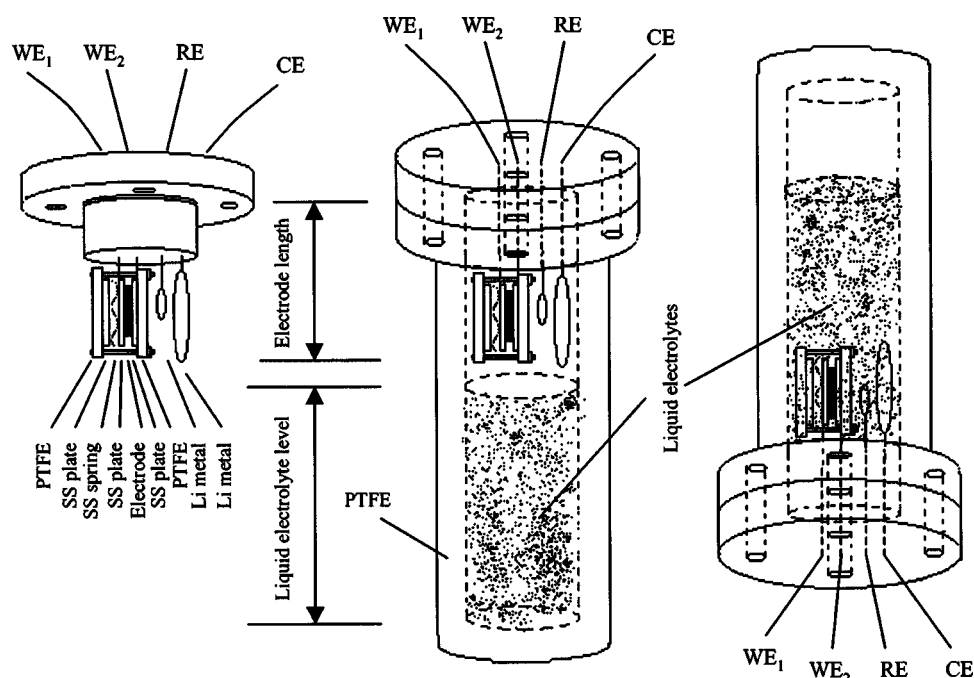


**Figure 1.** PTFE cell configuration designed for *in situ* electrical conductivity measurement of sintered  $\text{La}_{0.55}\text{Li}_{0.35}\text{TiO}_3$  disk electrode at different Li insertion levels without influence of liquid electrolytes. The ceramic electrode was charged-discharged in an inverted position, and then the electric conductivity was measured at the same Li insertion levels by EIS with the cell in an upright position.

change when it was charged/discharged on one side [working electrode (WE) side in Fig. 2] only.

**Structural and electrochemical measurements.**—The electrical conductivities of the sintered samples were measured over the frequency range 65 KHz to 0.01 Hz at a potentiostatic signal amplitude of 5 mV, using a frequency response analyzer (Solartron, FRA 1250) and an electrochemical interface (Solartron, model 1286). The crystal structure of the  $\text{La}_{0.55}\text{Li}_{0.35}\text{TiO}_3$  powder (calcined at 1100°C for 4 h) and the sintered  $\text{La}_{0.55}\text{Li}_{0.35}\text{TiO}_3$  disk were investigated using X-ray diffraction (XRD) with Cu K $\alpha$  radiation (D8 discover with Gadds, Bruker-AXS, Inc.).

### Results and Discussion

**X-ray diffraction structural analysis.**—Figure 3 shows the XRD patterns of  $\text{La}_{0.55}\text{Li}_{0.35}\text{TiO}_3$  powders and a sintered  $\text{La}_{0.55}\text{Li}_{0.35}\text{TiO}_3$  sheet coated with Au. The  $\text{La}_{0.55}\text{Li}_{0.35}\text{TiO}_3$  powders have a perovskite-type structure. A broadening of the superstructure lines (marked with arrows) was clearly observed. The XRD patterns of  $\text{La}_{0.55}\text{Li}_{0.35}\text{TiO}_3$  powders are in agreement with the previously reported XRD data of the ceramic with a similar composition.<sup>3</sup> The Au-coated  $\text{La}_{0.55}\text{Li}_{0.35}\text{TiO}_3$  sheet which was sintered at 1300°C for 4 h has the same phase as the  $\text{La}_{0.55}\text{Li}_{0.35}\text{TiO}_3$  powder calcined at 1100°C as shown in Fig. 3.

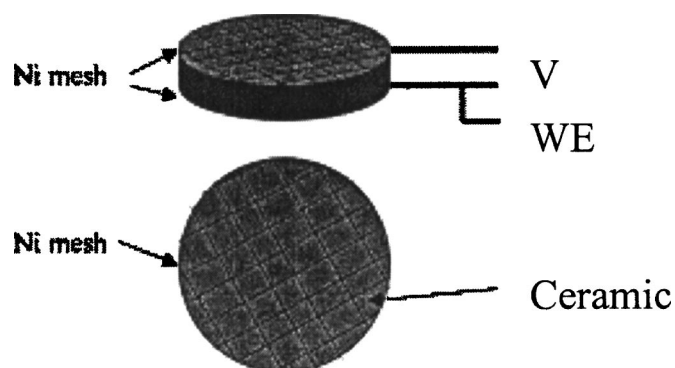


**Figure 2.** Schematic diagram of ceramic powder electrode configuration.

**Charge-discharge behavior of  $\text{La}_{0.55}\text{Li}_{0.35}\text{TiO}_3$  powder electrodes.**—Figure 4 shows the potential of operational current collector (WE in Fig. 2) and that of the unconnected current collector for the  $\text{La}_{0.55}\text{Li}_{0.35}\text{TiO}_3$  powder disk electrode on the first charge/discharge cycle at a current of 1 mA/g. Li atoms insert into  $\text{La}_{0.55}\text{Li}_{0.35}\text{TiO}_3$  below 1.0 V, a lower potential than that reported in the literature because of the high charge current. Only a small amount of inserted Li could be extracted when the electrode was charged to 0 V, in agreement with published results.<sup>4</sup> The potential on the unconnected side remained at 2.6 V during Li insertion up to 16.0 mAh/g, showing that  $\text{La}_{0.55}\text{Li}_{0.35}\text{TiO}_3$  is still a good Li-ion conductor and electronic insulator to this point. Upon further Li insertion, the potential of the unconnected side begins to decrease and the voltage across the electrode become smaller, suggesting that  $\text{La}_{0.55}\text{Li}_{0.35}\text{TiO}_3$  had then changed to a mixed conductor and finally to an electronic conductor.

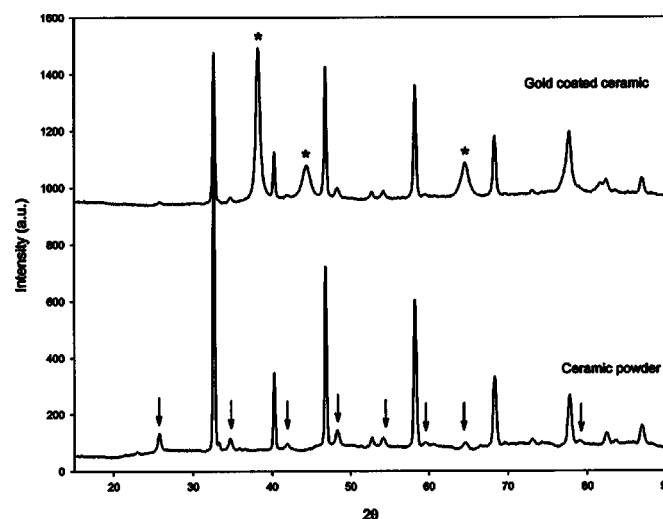


**Figure 3.** XRD patterns of  $\text{La}_{0.55}\text{Li}_{0.35}\text{TiO}_3$  powder and Au-coated  $\text{La}_{0.55}\text{Li}_{0.35}\text{TiO}_3$  sheet. Arrows denote superstructure peaks of the perovskite, and (\*) the Au line.

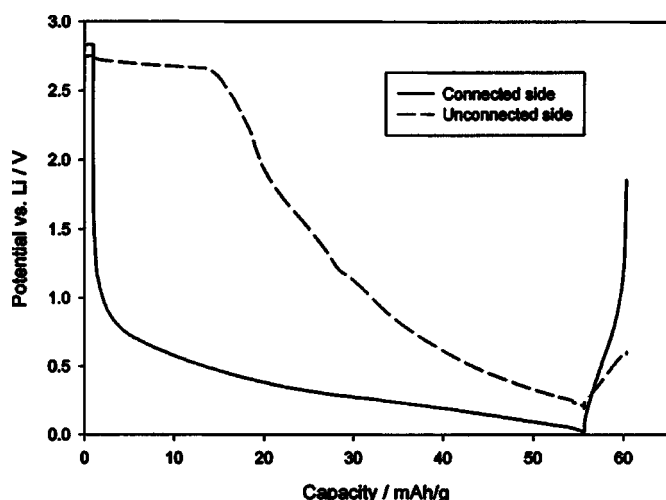


**Figure 4.** Potentials at the charge-discharge side and the unconnected side of  $\text{La}_{0.55}\text{La}_{0.35}\text{TiO}_3$  on the first Li insertion-extraction at 1.0 mA/g current.

To avoid the influence of electrochemical polarization on the trans-electrode voltage and Li insertion potential, galvanostatic intermittent titration (GITT) measurements were performed on the active current collector during the first Li insertion cycle into  $\text{La}_{0.55}\text{Li}_{0.35}\text{TiO}_3$  powder electrode (Fig. 5). In these measurements, the lithium was inserted into the electrode in a series of intermittent charge steps at a low current of 0.5 mA/g for 2.0 h, the electrode being left at open circuit for 2.0 h between each step to establish pseudoequilibrium. Meanwhile, the potential on the uncharged side was also recorded by computerized data acquisition. In Fig. 5, Li insertion into  $\text{La}_{0.55}\text{Li}_{0.35}\text{TiO}_3$  begins at 1.5 V and shows a potential plateau at a potential around 1.0 V, which is higher than that using a continuous galvanostatic cycling at high current density (1.0 mA/g). The potential behavior is in agreement with Chen's results using similar GITT measurements.<sup>4</sup> As under continuous galvanostatic charge/discharge conditions (Fig. 4), the potential on the unconnected side of the electrode was essentially stable at around 2.7 V before Li GITT insertion to 12 mAh/g (Fig. 5). It then gradually decreased to the same potential as that on the charging side, indicating the development of electronic conductivity. The overpotentials decreased only slightly with the Li insertion level, although the elec-

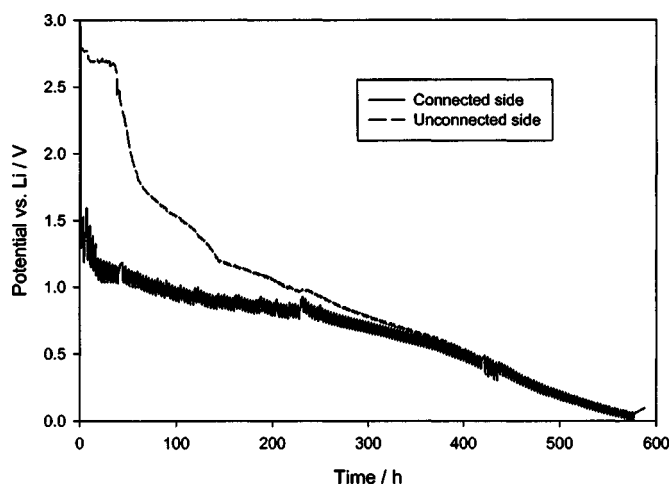


**Figure 5.** Potentials at the charging side and unconnected side as a function of time for the first Li insertion cycle in  $\text{La}_{0.55}\text{Li}_{0.35}\text{TiO}_3$  using GITT. Charge current 0.5 mA/g. The intermittent current was applied for 2.0 h, then switched off for 2.0 h.

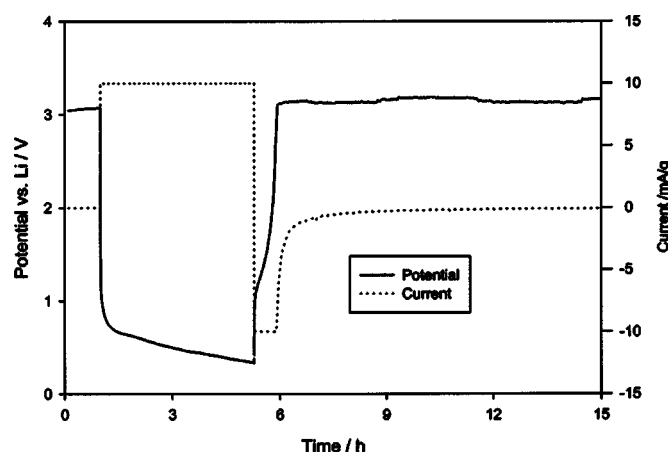


**Figure 6.** The dependence of the potential and current of  $\text{La}_{0.55}\text{Li}_{0.35}\text{TiO}_3$  powder electrode during charge (Li insertion) and discharge (Li extraction) in a liquid electrolyte between 0.33 and 4.2 V. Before charge/discharge, the electrode was at open circuit for 1 h.

trode changed from an electronic insulator to a conductor. It is interesting that an ionically conducting electronic insulator can be charged/discharged in the same way as a normal electrode. The possible mechanism for Li insertion into  $\text{La}_{0.55}\text{Li}_{0.35}\text{TiO}_3$ , an ionically conducting electronic insulator, can be described as follows.

Upon charging at a low potential, lithium is electrochemically inserted into  $\text{La}_{0.55}\text{Li}_{0.35}\text{TiO}_3$  particles that are physically contacting the Ni screen current collector. These Li inserted  $\text{La}_{0.55}\text{Li}_{0.35}\text{TiO}_3$  particles near the Ni screen change from electronic insulator to mixed conductor, which, in turn, enhances the Li insertion process. The fast Li diffusion in  $\text{La}_{0.55}\text{Li}_{0.35}\text{TiO}_3$  particles changes the whole particle to a mixed conductor and results in the lithium insertion into a neighboring  $\text{La}_{0.55}\text{Li}_{0.35}\text{TiO}_3$  in the same way as this particle. However, the electrical conductivity changes of  $\text{La}_{0.55}\text{Li}_{0.35}\text{TiO}_3$  powder electrode during discharge were quite different from that during the charging. On discharge,  $\text{La}_{0.55}\text{Li}_{0.35}\text{TiO}_3$  particles near the Ni screen current collector change from mixed conductor to electronic insulator on lithium extraction from them, and result in a decrease of discharge current even in galvanostatic cycling because the local area in contact with the Ni current collector becomes an electronic insulator. Figure 6 shows the potential and current profiles of a  $\text{La}_{0.55}\text{Li}_{0.35}\text{TiO}_3$  powder electrode which was galvanostatically charge/discharged at a current of 10 mA/g on both Ni current collector sides. As expected, the electronic insulator  $\text{La}_{0.55}\text{Li}_{0.35}\text{TiO}_3$  can be charged and discharged up to 3.1 V. When the potential of the  $\text{La}_{0.55}\text{Li}_{0.35}\text{TiO}_3$  powder electrode was over 3.1 V, the discharge current was gradually decreased to 0.00 as suggested by the supposed mechanism. This Li insertion/extraction mechanism can also explain the reason the Li extraction capacity of  $\text{La}_{0.55}\text{Li}_{0.35}\text{TiO}_3$  ceramic electrode is lower than that in Li insertion if cycling current is relatively high, as observed by Chen and Amine.<sup>4</sup> When electronic conducting carbon black is mixed into the  $\text{La}_{0.55}\text{Li}_{0.35}\text{TiO}_3$  powder electrode, lithium can be extracted from all ceramic particles that contacted the carbon black, which increase the discharge capacity. Actually, with addition of acetylene black, about 0.48 Li can be reversibly inserted into and extracted from  $\text{La}_{0.55}\text{Li}_{0.35}\text{TiO}_3$ , while only a little Li can be extracted from  $\text{La}_{0.55}\text{Li}_{0.35}\text{TiO}_3$  without carbon addition.<sup>4</sup>

*In situ electrical conductivity measurements on  $\text{La}_{0.55}\text{Li}_{0.35}\text{TiO}_3$  ceramic at different Li insertion levels uninfluenced by the presence of electrolyte.*—*In situ* ionic and electronic conductivity of  $\text{La}_{0.55}\text{Li}_{0.35}\text{TiO}_3$  in liquid electrolytes as a function of Li content can be measured using transmissive impedance.<sup>5</sup> However, the ionic conductivity thus obtained can only reflect the relative conductivity

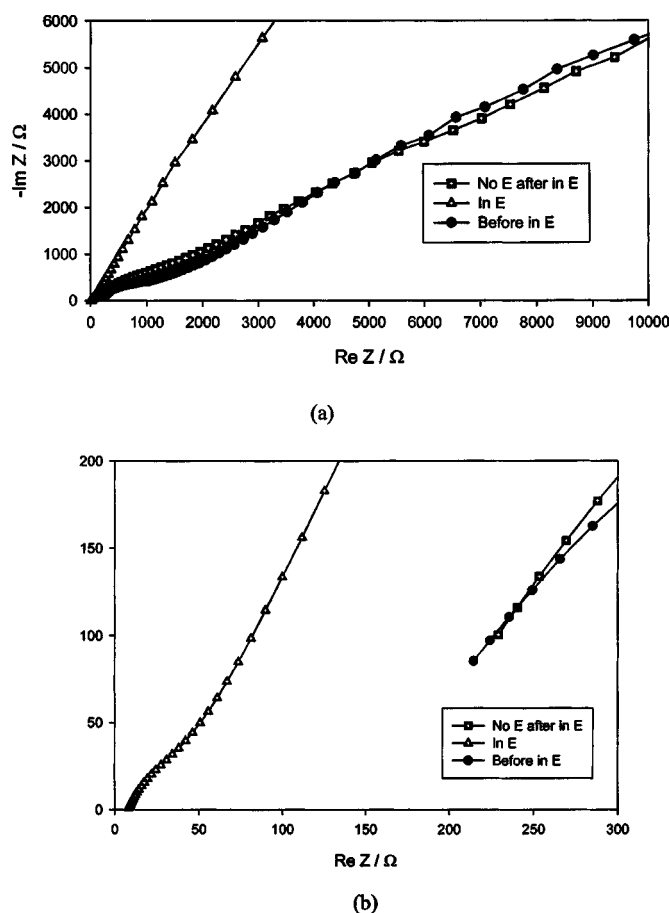


**Figure 7.** Impedances of sintered  $\text{La}_{0.55}\text{Li}_{0.35}\text{TiO}_3$  disk electrodes before immersion in electrolytes (before in E), during immersion (in E), and after immersion without electrolyte (cell upright, "No E after in E"). (b) A partial plot of (a) in the high-frequency range.

change as the Li content increases, because the conductivity of liquid electrolytes is much higher than that of the sintered  $\text{La}_{0.55}\text{Li}_{0.35}\text{TiO}_3$  sheet and the area of stainless steel holder is larger than that of the  $\text{La}_{0.55}\text{Li}_{0.35}\text{TiO}_3$  sheet, resulting in short-circuiting, giving a higher conductivity than the real value under an inert atmosphere. A special PTFE cell was therefore constructed with a sintered  $\text{La}_{0.55}\text{Li}_{0.35}\text{TiO}_3$  disk electrode and Li reference and counter electrodes, all suspended above a liquid electrolyte. Li insertion/extraction into or from  $\text{La}_{0.55}\text{Li}_{0.35}\text{TiO}_3$  was conducted in the liquid electrolyte with the cell in the inverted position, and the ionic conductivity of  $\text{La}_{0.55}\text{Li}_{0.35}\text{TiO}_3$  at each Li content was measured in the absence of liquid electrolyte with the cell upright. The influence of high-ionic-conductivity liquid electrolytes on the experimental ion conductivity of a fresh sintered  $\text{La}_{0.55}\text{Li}_{0.35}\text{TiO}_3$  disk electrode was determined by measuring EIS impedances before and during immersion in electrolyte by turning the cell from the upright to inverted position, followed by a further measurement without liquid electrolyte by turning the cell back to the upright position. The experimental impedances are shown in Fig. 7. All the impedance spectra consist of a semicircle in the high-frequency range and a straight line in the low-frequency range (Fig. 7a). The straight line is related to the lithium-ion diffusion in the  $\text{La}_{0.55}\text{Li}_{0.35}\text{TiO}_3$  electrode. Because the Li-ion diffusion in the liquid electrolytes is much faster than that in solid  $\text{La}_{0.55}\text{Li}_{0.35}\text{TiO}_3$  ceramic, the lithium-ion diffusion tends to shift from an infinite space to a finite space. Therefore, greater accumulation, which corresponds to a capacitive behavior, is involved for the electrode in the liquid electrolyte.<sup>4</sup> Hence, the angle of the straight line for ceramic immersed in liquid electrolytes is higher

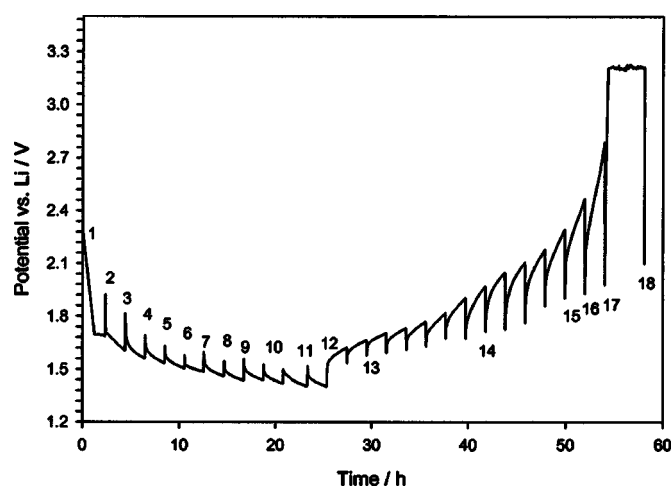


**Figure 8.** Charge-discharge profiles of a sintered  $\text{La}_{0.55}\text{Li}_{0.35}\text{TiO}_3$  disk electrode as a function of charge/discharge time using GITT. The charge current of 0.6 mA/g and discharge current of 0.5 mA/g were switched on for 2.0 h and off for 2.0 h before EIS measurement.

than that without liquid electrolyte. In addition, there is an intercept at the high-frequency end of the semicircle (Fig. 7b), which represents the ionic resistance of the  $\text{La}_{0.55}\text{Li}_{0.35}\text{TiO}_3$  electrode. The impedance spectra are typical for a pure ionic conductor with blocking electrodes and consistent with that observed by Chen and Amine.<sup>4</sup> The ionic conductivity of sintered  $\text{La}_{0.55}\text{Li}_{0.35}\text{TiO}_3$  before immersion in the liquid electrolyte was  $1.0 \times 10^{-3}$  S/cm. It increased to  $2 \times 10^{-2}$  S/cm after the disk sample was immersed in the liquid electrolyte by inverting the cell. The conductivity of  $\text{La}_{0.55}\text{Li}_{0.35}\text{TiO}_3$

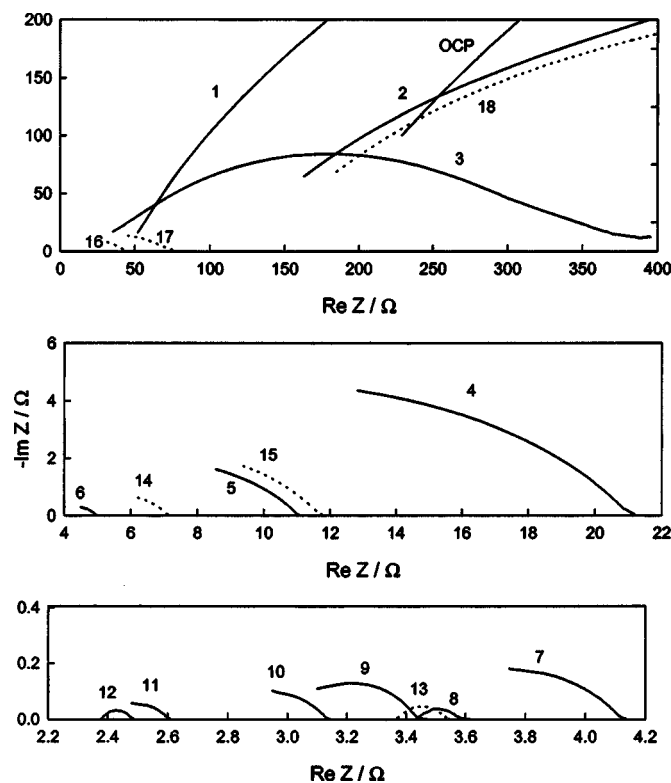


**Figure 9.** Impedance of the sintered  $\text{La}_{0.55}\text{Li}_{0.35}\text{TiO}_3$  disk electrode in Fig. 8 in the absence of liquid electrolyte: (—) charged state and (·····) discharged state.



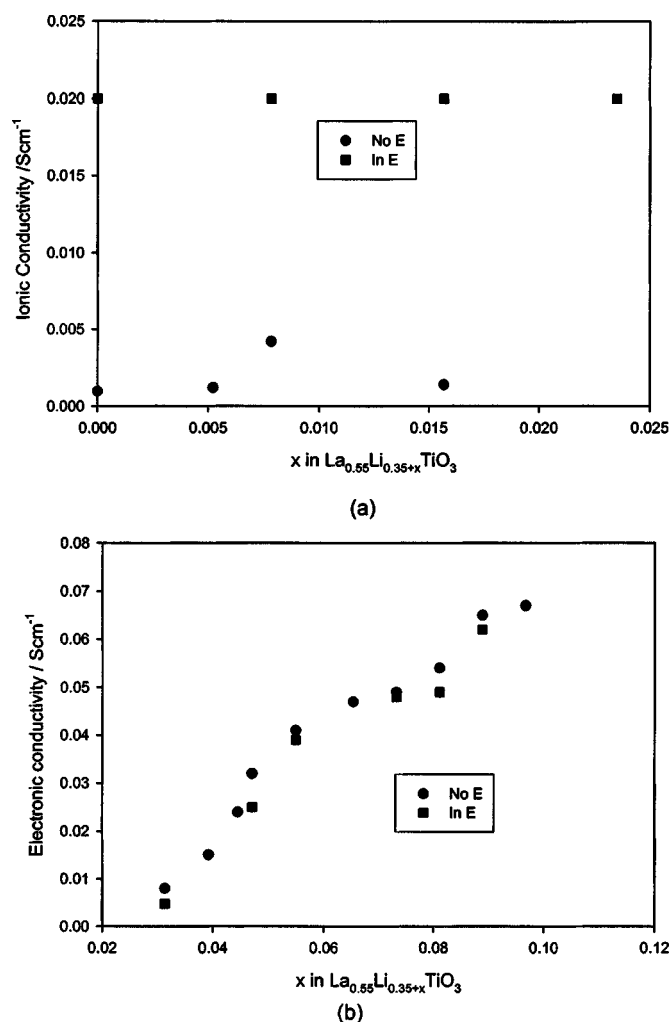


**Figure 10.** (a) Ionic and (b) electronic conductivities of a sintered La<sub>0.55</sub>Li<sub>0.35</sub>TiO<sub>3</sub> disk electrode as a function of Li intercalation levels using GITT.

in liquid electrolyte is almost 20 times higher than that before immersion into the liquid electrolyte. After removing the electrolyte by turning the cell back to the upright position, the Li-ion conductivity became  $0.96 \times 10^{-3}$  S/cm, which was similar to the conductivity before immersion in electrolyte. Thus, the specially designed PTFE cell provides a means of measuring the absolute conductivity of La<sub>0.55</sub>Li<sub>0.35</sub>TiO<sub>3</sub> at different electrochemically inserted Li levels in the absence of any influence of liquid electrolyte.

To investigate the conductivity of the La<sub>0.55</sub>Li<sub>0.35</sub>TiO<sub>3</sub> as a function of Li content, electrodes were charged/discharged in liquid electrolytes between 3.0 and 1.38 V with the cell inverted using GITT. Figure 8 shows the potential profile of a sintered La<sub>0.55</sub>Li<sub>0.35</sub>TiO<sub>3</sub> disk electrode during the initial Li insertion (0.6 mA/g) and extraction (0.5 mA/g) under these conditions. Impedances were measured at each Li content after 2.0 h at open circuit in the inverted and upright positions, *i.e.*, with and without electrolyte. Figure 9 shows the impedance of the sintered La<sub>0.55</sub>Li<sub>0.35</sub>TiO<sub>3</sub> disk electrode in the absence of liquid electrolyte with the cell upright. The ionic and electronic conductivities obtained from the EIS in Fig. 9 were plotted as a function of the lithium intercalation levels as shown in Fig. 10. After insertion, the Li<sup>+</sup> ion conductivity of the specimen is determined from the intersection of the high-frequency line with the real axis, first increasing and then decreasing (Fig. 10). The changes in ionic conductivity with Li insertion are in agreement with previously reported conductivity changes of La<sub>1.33-x</sub>Li<sub>3x</sub>Ti<sub>2</sub>O<sub>6</sub> ( $0.1 < x$

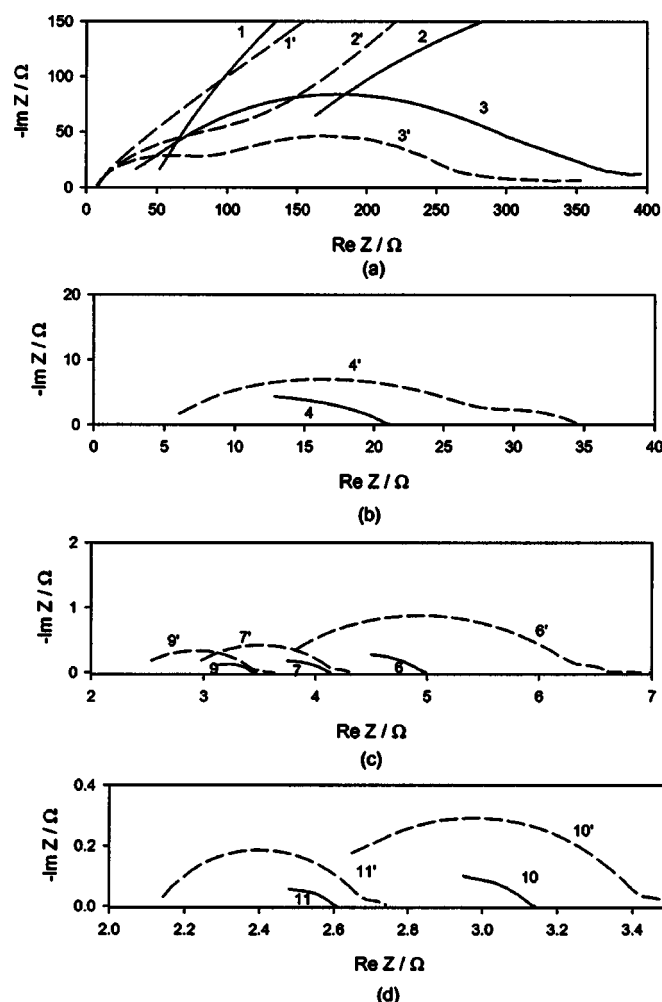


**Figure 11.** Impedance of the sintered La<sub>0.55</sub>Li<sub>0.35</sub>TiO<sub>3</sub> disk electrode in Fig. 8 with and without interference by liquid electrolyte: (—) without electrolyte and (---) immersed in electrolyte.

$< 0.3$ ) samples with different Li content.<sup>6</sup> Upon further lithium insertion, the capacitive behavior of the ionic conductor with blocking electrodes (Fig. 9) gradually changed to a depressed semicircle, which is characteristic of a mixed-conductor electrode.<sup>5</sup> The electronic conductivity can be obtained from the intersection of the low-frequency line with the real axis. The electronic conductivity of La<sub>0.55</sub>Li<sub>0.35</sub>TiO<sub>3</sub> ceramic progressively increased on electrochemical Li insertion (Fig. 10). Therefore, on Li insertion, the La<sub>0.55</sub>Li<sub>0.35</sub>TiO<sub>3</sub> ceramic changed from an ionic to an electronic conductor. Both Li insertion/extraction and the change in conductivity with Li content were reversible during GITT cycling between 1.3 and 3.1 V, as Fig. 8-10 show.

Because the liquid electrolyte is a Li-ion conductor but an electronic insulator, its influence on the electric conductivity of La<sub>0.55</sub>Li<sub>0.35</sub>TiO<sub>3</sub> at different Li insertion levels should change as it progresses from predominantly ionic to electronic conduction as Li content increased. Figure 11 shows the impedances of La<sub>0.55</sub>Li<sub>0.35</sub>TiO<sub>3</sub> with and without electrolyte at Li contents shown in Fig. 8. The ionic and electronic conductivities of La<sub>0.55</sub>Li<sub>0.35</sub>TiO<sub>3</sub> at different Li intercalation levels in liquid electrolyte are also shown in Fig. 10 for comparison. When the material is an ionic conductor (at a low Li content), the ionic conductivity in liquid electrolyte is much higher than that in its absence, because the ionic conductivity of liquid electrolytes is much greater than that of La<sub>0.55</sub>Li<sub>0.35</sub>TiO<sub>3</sub>. However, when La<sub>0.55</sub>Li<sub>0.35</sub>TiO<sub>3</sub> changed from ionic to ionic-

electronic mixed conductor (at high Li content), the mixed-electric conductivity of  $\text{La}_{0.55}\text{Li}_{0.35}\text{TiO}_3$  measured in electrolyte was lower than that in the absence of electrolyte. However, the difference in the conductivity of a  $\text{La}_{0.55}\text{Li}_{0.35}\text{TiO}_3$  electrode in and out of liquid electrolyte becomes smaller when the ceramic material changes from a mixed conductor to an electronic conductor during Li insertion. The low electronic conductivity of mixed-conductor  $\text{La}_{0.55}\text{Li}_{0.35}\text{TiO}_3$  in liquid electrolyte is possibly because the liquid electrolyte, an ionic conductor but electronic insulator, increased the ionic conductivity but decreased the electronic conductivity of the  $\text{La}_{0.55}\text{Li}_{0.35}\text{TiO}_3$  mixed conductor.

$\text{La}_{0.55}\text{Li}_{0.35}\text{TiO}_3$  is not electrochemically stable below 1.5 V. However, the stable window can be enlarged by insertion of a thin layer of stable solid electrolyte between the anode and the  $\text{La}_{0.55}\text{Li}_{0.35}\text{TiO}_3$  electrolyte to form a two-layer, lithium-ion-conducting solid electrolyte structure,<sup>7</sup> for example, by using a very thin PEO or  $\text{LiI-Li}_2\text{S-P}_2\text{S}_5$  film in contact with the anode material with  $\text{La}_{0.55}\text{Li}_{0.35}\text{TiO}_3$  contacting the cathode.

### Conclusions

Lithium can be electrochemically inserted into  $\text{La}_{0.55}\text{Li}_{0.35}\text{TiO}_3$  solid electrolyte, which results in a change of  $\text{La}_{0.55}\text{Li}_{0.35}\text{TiO}_3$  solid electrolyte from electronic insulator to electronic conductor during progressive Li insertion. The real electric conductivity of  $\text{La}_{0.55}\text{Li}_{0.35}\text{TiO}_3$  at different Li insertion levels (without the influence of liquid electrolytes) can be obtained by measuring the impedance

of  $\text{La}_{0.55}\text{Li}_{0.35}\text{TiO}_3$  which is suspended above a liquid electrolyte (with the cell in an upright position), after  $\text{La}_{0.55}\text{Li}_{0.35}\text{TiO}_3$  has been charged in the liquid electrolyte with the cell inverted. When  $\text{La}_{0.55}\text{Li}_{0.35}\text{TiO}_3$  is immersed in the high-ion-conductor liquid electrolyte, the liquid electrolyte increased the measured ionic conductivity of  $\text{La}_{0.55}\text{Li}_{0.35+x}\text{TiO}_3$  ceramic if  $\text{La}_{0.55}\text{Li}_{0.35+x}\text{TiO}_3$  is still an ionic conductor at a low Li insertion levels, but increased the electronic conductivity of  $\text{La}_{0.55}\text{Li}_{0.35+x}\text{TiO}_3$  if the  $\text{La}_{0.55}\text{Li}_{0.35+x}\text{TiO}_3$  becomes a mixed conductor at high Li insertion levels.

### Acknowledgments

We gratefully acknowledge NASA-Glenn Research Center (grant no. NAG3-2617) and the Welch Foundation grant no. V-1103 for supporting this work.

*Lamar University assisted in meeting the publication costs of this article.*

### References

1. C. Delmas, N. Nadiri, and J. L. Soubeyroux, *Solid State Ionics*, **28-30**, 419 (1988).
2. J. S. Yue, Y. Inaguma, and M. Itoh, *Solid State Ionics*, **79**, 245 (1995).
3. J. Ibarra, A. Varez, C. Leon, J. Santamaria, L. M. Torres-Martinez, and J. Sanz, *Solid State Ionics*, **134**, 219 (2000).
4. C. Chen and K. Amine, *Solid State Ionics*, **144**, 51 (2001).
5. C. Wang, A. J. Appleby, and F. Little, *J. Electrochem. Soc.*, **148**, A762 (2001).
6. A. I. Ruiz, M. L. Lopez, M. L. Veiga, and C. Pico, *Solid State Ionics*, **112**, 291 (1998).
7. K. Takada, T. Inada, A. Kajiyama, H. Sasaki, S. Kondo, M. Watanabe, M. Murayama, and R. Kanno, *Solid State Ionics*, **158**, 269 (2003).